Development of an On-Machine External Thread Measurement System for CNC Lathes Using Eye-in-Hand Machine Vision with Morphology Technology

Yi-Cheng Lee, Yu-Chen Wu, and Syh-Shiuh Yeh, *Member, IAENG*

Abstract—**Thread inspection is an important part of modern industrial inspection processes and the key to product quality. Traditional inspection methods, which are mostly of the contact type, are time consuming and expensive. Therefore, this study developed an automatic on-machine, non-contact measurement system for thread profiles by using eye-in-hand machine vision with morphology technology. On the basis of machine vision, this study proposed a method of measuring thread dimensions to implement non-contact, rapid, accurate measurements. The measurement samples were metric threads, and the images of thread profiles were obtained by backlight during the measurement process. Numerous image processing and machine vision methods were developed to analyze the thread images and thread profiles and calculate the depth and pitch of threads. This study also clarifies the steps involved in the selection of the imaging system, hardware settings, image capture, and information processing for the measurement system. The developed system-measured dimensions and 3D microscope-measured target dimensions were compared and validated. Results showed that the maximum difference between the target and measured dimensions was 6 μm (one pixel). The measurement difference for the three workpiece samples was approximately two pixels, thereby validating the feasibility and accuracy of the system and the approaches used in this study.**

Index Terms—**CNC lathes, eye-in-hand, external threads, machine vision, morphology technology, on-machine measurement**

I. INTRODUCTION

NOWADAYS, engineering technology is changing rapidly due to various manufacturers constantly improving their product quality and manufacturing efficiency. Product dimension inspections are an important part of the production flow, and they are crucial in the inspection of thread dimensions. At present, thread measuring devices used in industrial circles, such as three-wire thread gauges, screw-thread pitch gauges, and screw-thread micrometers, are generally of the contact type. The measurement ranges and measurement approaches of these measuring devices are inapplicable to small threads where manual measurement is required. Therefore, overall inspections cannot be performed using automated methods. General thread measuring methods use various measuring devices and approaches in accordance with different inspection parameters. Thread inspection parameters include thread depth, thread pitch, major diameter, minor diameter, and pitch diameter, with different devices being used to inspect individual parameters. The use of individual inspections has resulted in time-consuming and inconvenient measurements. Furthermore, the inspected object must be moved to the inspection devices for different inspection parameters, leading to unnecessary manual inspection errors. The merits of using a computer vision system for non-contact thread measurement include the following: simultaneous measurements of multiple parameters, small threads can be measured because the process is not limited to the dimensions of the measuring devices, and online measurement is available during the production run, thereby reducing labor costs and facilitating automated quality control. The purpose of this study is to use non-contact computer vision methods to develop a measurement system suitable for on-machine thread dimension inspection.

Image recognition and dimensional measurement are among the major machine vision trends. Most current studies that use machine vision for thread measurement and inspection target offline applications; on-machine thread measurement has seldom been studied. In addition to studies on offline external thread image inspection, the current work refers to other external offline thread inspection methods. Studies on thread measurement are conventionally divided into on-machine image-based measurements of thread dimensions, offline image-based measurements, and offline non-image-based measurements. With regard to studies on offline non-image-based measurements of thread dimensions, Lin et al. used laser triangulation for real-time pitch diameter measurements of the internal threads of a nut [1]. Lavrinov and Khorkin proposed a signal processing method with laser triangulation by using a 2D scanner for high-quality thread pitch measurement [2]. Tong et al. developed a new type of

Manuscript received October 8, 2020; revised May 3, 2021. This research was supported in part by the Ministry of Science and Technology, Taiwan, under contracts MOST107-2221-E-027-108 and MOST107-2218-E-009 -59.

Y. C. Lee is a graduate student of the Institute of Mechatronic Engineering, National Taipei University of Technology, Taipei 10608, Taiwan (e-mail: andy11366@yahoo.com.tw).

Y. C. Wu is a PhD student of the Institute of Mechatronic Engineering, National Taipei University of Technology, Taipei 10608, Taiwan (e-mail: paul810226@gmail. com).

S. S. Yeh is an Associate Professor of the Department of Mechanical Engineering, National Taipei University of Technology, Taipei 10608, Taiwan (phone: +886-2- 27712171; fax: +886-2-27317191; e-mail: ssyeh@ntut.edu.tw).

laser measurement system to measure internal thread parameters [3]. Lin et al. proposed a design and characterization analysis method based on a laser inspection system [4]. Huang et al. developed a new type of laser measurement system for ball screw-thread profiles [5]. Zhao et al. proposed the metrology of a conical thread gauge [6]. Maciel et al. discussed the characteristics of titanium alloy machining and forming of external threads [7]. Leun and Nikolaeva proposed cutting and monitoring tools to measure the mean thread diameter of thread grinding [8, 9]. Wu et al. proposed the study of and software development for a thread measurement algorithm [10]. Sheng et al. developed a compensation method using profile scanning to measure the thread pitch diameter [11]. Kosarevsky and Latypov proposed a thread inspection method for computed tomography 3D density fields [12]. Hong et al. proposed non-contact type inspection for the internal threads of machined parts [13]. Cheng et al. presented an enhanced, high-accuracy, non-contact type system for measuring the geometric dimensions of irregular shapes [14]. Shchurov used the cloud of points from a coordinate measuring machine to calculate the virtual pitch thread diameter [15]. Merkač and Ačko proposed a thread gauge calibration method for industrial applications [16]. Kosarevsky and Latypov developed an algorithm for the inspection of screw threads in planar point clouds [17]. Gadelmawla introduced a new measurement system for the automatic measurement and inspection of parallel screw threads [18]. Hunsicker et al. presented an automatic visual inspection and measurement system for external threads [19]. Corley et al. proposed a direct-contact profile characterization method for thread surfaces [20].

With regard to studies on offline and on-machine image-based measurements of thread dimensions, Senthilnathan et al. proposed metric screw-thread parameter orientation-invariant measurement based on a visual method [21]. Gadelmawla introduced computer vision algorithms for the measurement and inspection of external threads [22]. Chao and Zhang presented an intelligent detection method and thread image capture and information processing process in which non-contact, rapid, accurate measurements of small pitch thread parameters can be implemented [23]. Zhao et al. proposed a new type of non-contact measurement system that uses a charge-coupled device camera, which measures the thread profile and features of ball screws of different sizes and lengths [24]. However, current thread dimension measurement systems have numerous practical application problems. These measurement systems cannot move to the actual machining environment inside computer numerical control (CNC) lathes; therefore, they cannot be effectively used for automatic thread dimension measurements and inspection of a production line. In addition, these measurement systems do not consider the practical application problems of camera protection and installation, leading to complex installation processes, inconvenience, and limited operation of CNC lathes. Furthermore, such measurement systems cannot capture effective thread images and features due to the adhesion of cutting fluid and chips.

Recently, scholars used a manipulator to develop an eye-in-hand, on-machine thread dimension measurement system with a simple structure that can be rapidly integrated with a CNC lathe for thread dimension measurement and inspection [25]. This approach uses a manipulator to increase the measurement degrees of freedom (DOF) and capture high-quality thread images and features. However, the measurement results are considerably affected by the image processing methods used to obtain image features. The thread dimension measurement process developed in this study comprises image pre-processing, image analysis, and dimension calculation stages to improve the quality of obtained features and further enhance the measurement results. At the image pre-processing stage, the measurement system captures thread images and trims the region of interest (ROI) for the horizontal calibration of the images. At the image analysis stage, the measurement system performs image smooth filtering, binarization, closing morphology, and thread edge detection. At the dimension calculation stage, the measurement system obtains the thread profile and feature points then calculates the thread dimensions in accordance with the feature points. In addition, this study used the Taguchi method to design optimal image processing parameters for obtaining stable and accurate thread dimension calculation results. This study implemented the developed measurement system and methodologies in a CNC lathe to compare the measured dimensions with 3D microscope-measured target dimensions. The experimental results showed that the maximum difference between the target and measured dimensions was approximately 6 μm (one pixel), and the measurement difference for the three workpiece samples was approximately two pixels. The experimental results validated the feasibility and accuracy of the measurement system and the approaches developed in this study.

The structure of this paper is described as follows. The experimental equipment used in this study, including the integrated structure of the CNC lathe and manipulator, hardware design, and installation related to the measurement system, are described in Section 2. The thread image processing procedures, including thread image capturing, ROI trimming, horizontal calibration of images, smooth filtering and binarization of images, closing morphology, and thread edge detection, are described in Section 3. Section 4 presents the thread dimension calculation methods, including thread profile and feature point acquisition, feature point position calculation, and thread dimension calculation. Section 5 describes the design processes of the optimal image processing parameters using the Taguchi method, the comparative experimental results of the measurement system, and the approaches developed in this study to validate their feasibility and accuracy. The conclusions are presented in Section 6.

II. EXPERIMENTAL INSTRUMENTS AND SYSTEM STRUCTURE

This section introduces the thread workpiece samples measured in the experiment, the CNC lathe and manipulator, and the thread dimension measurement system developed in this study. The workpiece material measured in this experiment was S45C medium carbon steel. The measured workpiece sample is shown in Fig. 1. The experimental results were obtained from the front-end threads of the sample. The crest and root of the front-end threads of the sample corresponded to the crest and root in the thread image, respectively, as shown in Fig. 2.

This study used a GigE DFK 23GP031 color industrial camera, as shown in Fig. 3. The maximum image resolution was 2592×1944 pixels, and the maximum frame rate at this resolution was 15 fps. A high frame rate was required because this study targeted on-machine measurements of workpiece thread dimensions. A camera with high resolution, high frame rate, and a Myutron HS3514J CCTV lens was utilized. An extension tube was used to overcome the limitations in the field of view (FOV) and shooting distance inside the lathe, and a double lens satisfied the capture requirements of the featured images. The lens was provided with an additional 90° reflection mirror due to the working space limitations inside the CNC lathe. The reflection mirror could adjust the angle of the shot to implement a parallel configuration of the camera and workpiece. To shorten the computation time and increase the dimension measurement accuracy, this study used a reduced resolution of 1280×720 pixels, and the frame rate was increased from 15 fps to 25 fps. For measurements inside the CNC lathe, a protection box was designed to protect the camera. In consideration of the internal working space dimensions of the CNC lathe, a protection box with dimensions of 20×20×10 cm^3 was designed. By means of a double-layered aluminum shell, the protection box prevented the cutting fluid and chips stemming from the machining processes of the CNC lathe from hindering the lens.

Generally, given that threads are metals, the surface reflects light, and the threshold values are miscalculated in the image binarization process. Therefore, the installation of a light source has to be considered in the image capturing process to capture good thread images. Consequently, this study placed a light source on the other side of the camera to irradiate the threads, such that the light reflected onto the back side of threads and reduced the effect of thread surface reflection. The light source was an LED light strip with an adjustable light intensity. This study extended the light source to a light source module outside the protection box, fixing it to the slot of the fixture. A parallel configuration of the camera and workpiece was designed, and a parallel light source was used to measure the thread dimensions, as shown in Fig. 4.

Fig. 5 presents the structure of the manipulator and machine vision component inside the lathe during the actual measuring process. The system developed in this study measures the thread dimensions when the workpiece is on the spindle. The operational flows of the manipulator and machine vision component of the thread dimension measurement system developed in this study are as follows:

- The CNC lathe stops machining, and the protection door is opened.
- The thread surface is cleaned, and the manipulator is actuated to move the machine vision component into the lathe.
- The light source and camera protection window are activated.
- The light intensity of the light source is adjusted before the thread images are captured.
- Image pre-processing, image analysis, and dimension calculation are performed for the captured thread images.
- Thread dimension measurement is completed, and the manipulator is actuated to move the machine vision component out of the lathe for the machining of the next workpiece.

III. Thread Image Processes

Metric threads make up the thread standard formulated by the International Organization for Standardization. The size of the thread is represented by its nominal diameter or major diameter and thread pitch dimension; its units are mm. The metric thread follows the international metric thread system. The crest is produced using lathe machining, and the root is cambered to increase the thread strength. The thread angle is 60°. The thread specifications are represented by M; for example, M8×1.25, where M is the code, 8 is the nominal diameter, and 1.25 is the thread pitch. The names of different thread regions are shown in Fig. 6, and the basic specifications of the threads are shown in Fig. 7 [26]. Here, P represents the thread pitch, $H = 0.866P$, and $H_1 = 0.65P$. For the measurement of the thread dimensions in this study, P and H_1 in Fig. 7 were measured.

The thread dimension measurement process comprised image pre-processing, image analysis, and dimensional calculations. The measurement system captured the thread images. The ROIs in the images were trimmed and horizontally calibrated. Next, the measurement system performed smooth filtering, binarization, closing morphology, and thread edge detection. Then, the measurement system obtained the thread profile and positions of the feature points to calculate the thread dimensions. To enhance the contrast between the thread and image backgrounds, this study used a backlighting approach comprising a back parallel light source. A high-intensity light source was adopted to obtain satisfactory thread images, such that subsequent image processing and analysis were implemented rapidly and easily. After the images were captured, the measurement system trims the ROI of the thread images. If the ROI is untrimmed, the subsequent binarization process will become difficult, and the thread dimension calculation results will be affected. Horizontal calibration of the image can be performed after the trimming of image ROI. If the image is not horizontal and exhibits angular deflection, the positions of feature points will be incorrect when calculating the thread dimensions, leading to errors. This study designed a horizontal calibration method to establish the first and third crest positions, as shown in Fig. 8; the two positions were then connected to form a crest line. The included angle between the crest line and horizontal line was calculated, and the image was rotated to the horizontal plane, thereby completing horizontal image calibration.

After the completion of horizontal image calibration, Gaussian filtering was used to filter and reduce noise. Gaussian filtering is a smooth filtering process that is extensively used in noise reduction processes for image processing [27]. Generally, Gaussian filtering adopts a weighted average of the full image; the grayscale value of each pixel is obtained after calculating the weighted average of the grayscale value of itself and other pixels in the neighboring regions. Specifically, a filter kernel is used to scan the pixels in the image and calculate the weighted average grayscale value of pixels in the neighboring region to replace the grayscale value of the filter kernel's center pixel. Two general approaches are used for Gaussian filtering in image processing: use of the filter kernel and captured image for convolution and/or use of Fourier transform. The most common approach is to use filter kernel convolution. The weighted average is obtained by multiplying the grayscale value of a pixel with different coefficients, and a large coefficient provides a large weight for the pixel during calculation. The filter kernel size is the adjustable parameter for Gaussian filtering, and the common sizes are 3, 5, and 7. Therefore, this study used the three filter kernel sizes.

The image binarization process was performed after Gaussian filtering. To set the binarization threshold value, this study used the Otsu threshold value determination process [28]. In the Otsu threshold value determination process, the image histogram is calculated, pixels with a histogram grayscale value larger than the preset threshold are classified as a group, and pixels with a grayscale value smaller than the preset threshold value are classified as another group. The numerical data variance of the two groups of histograms is calculated, and the calculated variances are added to obtain the sum of variance. Grayscale values from 0 to 255 are sequentially set as the preset threshold value to calculate the corresponding sum of variance. The preset threshold value with the minimum sum of variance is defined as the Otsu threshold value. The limitation of the Otsu threshold value process is that the binarization processing effect is poor when there is no significant difference between the target object and image background. Therefore, this work used six threshold values for the experimental study (i.e., Otsu-40, Otsu-20, Otsu, Otsu+20, Otsu+40, and Otsu+60) to determine the optimal binarization threshold values.

After the binarization process, morphology operations are performed on the post-binarization images. The morphology uses a closing operation (dilation of the image before erosion) to smoothen the thread images. The voids and broken lines in the thread images are filled to make complete thread object images. Considering Sets A and B in space, when Set A is dilated by Set B, it is represented by $A \oplus B$ [29]. If A is the input image and B is the structuring element and if more than one of the grayscale values of the input pixel and peripheral pixels of 1 corresponding to the structuring element are 255, then the grayscale value of the input pixel is set as 255. The image will appear to be expanded as a result of the dilation operation. Therefore, dilation is generally used to fill the gaps. The dilation operation enhances the edge of thread object images and used appropriate structuring elements that can fill the gaps in the thread object images. Considering Sets A and B in space, when Set A is eroded by Set B, it is represented by $A \ominus B$ [29]. If A is the input image and B is the structuring element and if the grayscale values of the input pixel and peripheral pixels of 1 corresponding to the structuring element are 255, then the value of the input pixel is set as 255. The image will appear to be contracted as a result of the erosion operation. Therefore, the erosion operation uses appropriate structuring elements to eliminate noise in the images. The parameters to be set in the morphology operations include the template shape, template size, and number of operations. The template shapes include rectangles, crosses, and ellipses. The common template sizes are 3, 5, and 7. The number of operations is determined in accordance with the application and requirements. In this study, the template shapes were rectangles, crosses, and ellipses, and the template sizes were 3, 5, and 7. The numbers of operations were 3, 5, and 7.

After morphology operations, edge detection is performed on the thread images. This study used Canny edge detection to detect the thread profiles in the thread images. The steps of Canny edge detection operation include the use of Gaussian filtering to remove noise, computing the image intensity gradient magnitude and direction, and eliminating non-edge pixels [30, 31]. The adjustable parameters in the edge detection process include the maximum and minimum threshold values. If the intensity gradient of a pixel is higher than the maximum threshold value, then the pixel is regarded as an edge pixel; if the intensity gradient of a pixel is lower than the minimum threshold value, then the pixel is regarded as a non-edge pixel. If the intensity gradient of a pixel is between the maximum and minimum threshold values, then it is classified as either an edge pixel or a non-edge pixel according to the connectivity of the edge pixels. Generally, the ratio of the maximum threshold value to the minimum threshold value is 2:1–3:1. The maximum threshold value for Canny edge detection in this study was 600, and the minimum threshold value was 300. An image after Canny edge detection is shown in Fig. 9. After edge detection, segmentation, identification, and analysis of the thread images were performed to calculate the thread pitch and depth.

IV. Calculation of Thread Dimensions

After edge detection, the thread profiles of full thread images are determined in accordance with the detected thread edges to determine the positions of feature points and calculate the thread dimensions. As shown in Fig. 10, this study separated the thread profiles into four thread segments and calculated the depth of each thread segment and pitch of adjacent thread segments.

The positions of feature points for calculating the thread dimensions were identified in the four thread segments. Two approaches were used: the H_1 approach for finding the thread depth and the P approach for finding the thread pitch. For the calculation of H_1 (thread depth), the positions of feature points with a minimum Y value and a maximum Y value in the thread profile were established, and the vertical distance between positions of the feature points with a minimum Y value and positions of the feature points with a maximum Y value was calculated to obtain the thread depth. For the calculation of P (thread pitch), the feature points with a maximum Y value (Y_{Max}) in the thread profile were established, as shown in Fig. 11. The X-coordinate mean value X_M of all Y_{Max} feature points was calculated to obtain the position of the feature point (X_M, Y_{Max}). Then, the distance of the (X_M, Y_{Max}) feature point positions of the adjacent thread segments was calculated to obtain the thread pitch. This study further set Y-m value ($Y_{Max\text{-}m}$) feature points, as shown in Fig. 11. Similarly, the X-coordinate mean value $X_{M\text{-}m}$ of all Y-m feature points was calculated to obtain the feature point position ($X_{M\text{-}m}$, $Y_{Max\text{-}m}$). Then, the distance of the ($X_{M\text{-}m}$, $Y_{Max\text{-}m}$) feature point positions of the adjacent thread segments was calculated to obtain the thread pitch. As shown in Fig. 11, when $m = 5$, given that the Y-5 feature points are divided into two parts, the mean value $X_{U\text{-}5}$ of the upper feature points and the mean value $X_{L\text{-}5}$ of the lower feature points must be calculated. Then, the mean value of the X-coordinate mean value (i.e., $X_{M\text{-}5}$) as the mean of $X_{U\text{-}5}$ and $X_{L\text{-}5}$ was calculated. This study designed m as a variable value that affects the calculation results of the thread dimensions; therefore, an experiment was performed to determine the optimal m value.

The positions of the feature points for calculating the thread dimensions were established, and the pixel value of feature point positions was calculated before the physical quantities of the thread dimensions were calculated and converted. Given that the pixel value obtained by calculating the thread dimensions could not represent the physical values of the thread dimensions, the measurement system must convert the dimensions from units of pixels to μm. The conversion of the dimensions of P (thread pitch) is shown in Fig. 12, where A is the pixel distance between the positions of feature points Q_1 and Q_2 of the adjacent thread segments. The conversion of the dimensions of H_1 (thread depth) is shown in Fig. 13, where B is the pixel distance between the positions of feature points Q_1 and Q_3 of the thread segment. PU (pixel unit) is the conversion gain, i.e., $1\,\text{pixel} = K\ \mu\text{m}$, where the K value varies with FOV and image resolution. The K value in this study was 6.224. In other words, the size of each pixel in the thread images was equal to a physical dimension of 6.224 μm.

V. EXPERIMENTAL RESULTS

This study used the Taguchi method to design optimal image processing parameters for calculating the thread dimensions. The measured dimensions were compared with the target dimensions measured by using a 3D microscope to validate the feasibility and effectiveness of the thread dimension measurement system developed in this work. Figs. 14 and 15 show the thread pitch and thread depth, respectively, measured using a 3D microscope. The FOV of the thread dimension measurement system covered the frames shown in Figs. 14 and 15 due to the captured image resolution. The thread pitch (P_1, P_2, and P_3) measured using the thread dimension measurement system designed in this study corresponded to the thread pitch ($[1], [2], [3]$) measured using a 3D microscope shown in Fig. 14. The thread depth (H_1_1, H_1_2, H_1_3, and H_1_4) of the measurement system corresponded to the thread depth ($[1], [2], [3], [4]$) measured using a 3D microscope shown in Fig. 15. Fig. 16 shows the thread pitch (P_1, P_2, and P_3) and thread depth (H_1_1, H_1_2, H_1_3, and H_1_4) measured using the thread dimension measurement system.

The Taguchi method considers the factors used in this study, including binarization threshold values (T-hold), filter kernel size of Gaussian filtering (GF-Size), m value determining the positions of feature points (M-val), morphology template shape (MT-Shape), morphology template size (MT-Size), and morphology number of operations (MN-Times). The levels of T-hold were Otsu-40, Otsu-20, Otsu, Otsu+20, Otsu+40, and Otsu+60. The levels of GB-Size were 3, 5, and 7. The levels of M-values were 3, 4, and 5. The levels of MT-Shape were R (rectangle), C (cross), and E (ellipse). The levels of MT-Size were 3, 5, and 7. The levels of MN-Times were 3, 5, and 7. The $L_{18}(6^1 \times 3^5)$ orthogonal array of the Taguchi method is shown in Table I. The experiment and analysis were performed on the 18 groups of image processing parameters in the orthogonal array. Optimal image processing parameters were obtained, where T-hold was Otsu-40, GB-Size was 7, M-val was 3, MT-Shape was C (cross), MT-Size was 5, and MN-Times was 7.

Table II shows a comparison of the error between the system measured dimensions and the target dimensions measured using a 3D microscope. Error e was calculated with (1), where the system measured dimension ($Meas_{system}$) of the workpiece sample is subtracted from the target dimensions ($Meas_{microscope}$) of the workpiece sample measured using a 3D microscope to obtain the absolute value.

$$e = \left| Meas_{system} \text{-} Meas_{microscope} \right| \tag{1}$$

The average μ and standard deviation σ were calculated as (2) and (3), respectively.

$$\mu_P = \frac{1}{10}\sum_{i=1}^{10} e_i^{P\_j} \ \text{and} \ \mu_H = \frac{1}{10}\sum_{i=1}^{10} e_i^{H_1\_k} \tag{2}$$

$$\sigma_P = \sqrt{\frac{1}{10}\sum_{i=1}^{10}\left(e_i^{P\_j} - \mu_P\right)^2} \ \text{and} \ \sigma_H = \sqrt{\frac{1}{10}\sum_{i=1}^{10}\left(e_i^{H_1\_k} - \mu_H\right)^2} \tag{3}$$

The SN ratio was calculated using (4). Experimental results $e_i^{P\_j}$ and $e_i^{H_1\_k}$ represent the No. j thread pitch error and the No. k thread depth error of the No. i experiment, respectively.

$$SN = -10 \cdot log_{10}\left\{\frac{1}{10}\sum_{i=1}^{10}\left[\frac{1}{3+4}\left(\sum_{j=1}^{3} e_i^{P\_j} + \sum_{k=1}^{4} e_i^{H_1\_k}\right)\right]^2\right\} \quad (4)$$

Table II shows that the SN ratio of the 10 experimental results was −3.610. The maximum value of the average of H_1_2 was 5.400 μm. The minimum value of the average of P_2 was 0.269 μm (with a standard deviation 0.219 μm). The experimental results showed that the thread dimension measurement system developed in this study exhibited high accuracy and stability.

Three other workpiece samples were measured in this study, and the photograph and measurement results are shown in Fig. 17 and Table III, respectively. Table III shows the measurement results of the three workpiece samples, including the average (AVG), difference of average (DA), and ratio of DA (RDA) of the measured thread pitch and measured thread depth. AVG refers to the average of the thread dimension measurement results of the three workpiece samples. DA refers to the maximum absolute value obtained by subtracting the thread dimension measurement result of the three workpiece samples from AVG. RDA refers to the percentage after DA is divided by the AVG value. According to the measurement results in Table III, the minimum DA of P_3 was 4.698 μm, and the maximum DA of H_1_1 was 12.792 μm. Table III shows that the RDA of the measurement results was approximately 1%, proving that the measurement system of this study produced consistent measurement results. In addition, in comparison with the measurement of P, the measurement of H_1 had larger DA values because the cutting conditions and machining process of the workpiece samples resulted in large changes in thread depth. However, the measurement results showed that the DA values were approximately two pixels.

VI. Conclusion

Measurements of the final workpiece dimensions in production lines are important. In consideration of the environment and installation problems in on-machine thread dimension measurements of a CNC lathe, an eye-in-hand on-machine thread dimension measurement system was developed in this study. A manipulator was used to increase the measurement DOF of the system, such that the thread images and features could be captured for inspection and analysis. Conventionally, workpiece thread dimension measurement processes are performed using manual methods. Given that traditional measurement methods often reduce manufacturing efficiency and increase production costs, image measurement systems with high speed and high-accuracy measurement characteristics have attracted much attention. Therefore, this study developed an on-machine thread dimension measurement system based on machine vision methods.

The on-machine thread dimension measurement system developed in this study uses Microsoft Visual Studio C# and the Emgu CV library package to program computation and image processing methods. The designed system with a simple structure can be integrated with CNC lathes rapidly and conveniently. A protection box protects the camera against the machining processes of the CNC lathe. The measurement system performs spindle positioning and cleans the workpiece surface. The vision module and light source are moved by the manipulator to the measurement position for light source adjustments and to capture images. In terms of image processing, the measurement system trims the ROI in the thread images and performs horizontal calibration of the images, smooth filtering of the images, binarization, and closing morphology processing. Then, thread edge detection is performed to obtain the thread profile, and the thread pitch and thread depth are calculated. This study used the Taguchi method to determine the optimal image processing parameters for subsequent image processing and calculation of the thread dimensions, including the binarization threshold values, filter kernel size of Gaussian filtering, value determining the positions of the feature points, morphology template shape, morphology template size, and morphology number of operations. Experiments were performed on a CNC lathe, and the difference between the thread dimensions calculated using the measurement system and those measured using a 3D microscope was estimated to validate the feasibility of the on-machine thread dimension measurement system. The experimental results showed that the maximum value of average errors between the dimensions measured by the measurement system and those measured by the 3D microscope was 5.400 μm, and the minimum value was 0.269 μm. With regard to the measurement of the three other workpiece samples, the difference of the average of the measurement results was approximately two pixels, and the ratio of difference in average was approximately 1%. The experimental results validated the accuracy and stability of the measurement system developed in this study.

Acknowledgment

The authors would like to thank Prof. Ching-Yuan Chang (NTUT, Taiwan), Dr. Po-Huang Shieh, and Dr. Chao-Choung Mai (ITRI, Taiwan) for their helpful discussions.

References

[1] C. F. Lin, C. H. Hwang, H. R. Fang, C. Y. Chen, and J. R. Sze, "Real-time pitch diameter measurement of internal thread for nut using laser triangulation," in *Proc. 2017 IEEE International Instrumentation and Measurement Technology Conference,* 2017.

[2] D. S. Lavrinov and A. I. Khorkin, "Laser triangulation 2D scanner signal processing for premium thread pitch measurement," in *Proc. 2017 International Conference on Industrial Engineering, Applications and Manufacturing,* 2017.

[3] Q. B. Tong, B. Z. Han, D. L. Wang, J. Q. Wang, Z. L. Ding, and F. Yuan, "A novel laser-based system for measuring internal thread parameters," *Journal of Russian Laser Research,* vol. 35, no. 3, pp. 307–316, 2014.

[4] Y. C. Lin, P. H. Hu, K. Y. Huang, Y. H. Wang, S. S. Ko, and C. S. Liu, "Design and characterization of laser-based inspection system," in *Proc. 51st Annual Conference of the Society of Instrument and Control Engineers of Japan,* 2012, pp. 1062–1066.

[5] H. L. Huang, W. Y. Jywe, C. H. Liu, L. Duan, and M. S. Wang, "Development of a novel laser-based measuring system for the thread profile of ballscrew," *Optics and Lasers in Engineering,* vol. 48, no. 10, pp. 1012–1018, 2010.

[6] Y. Zhao, X. Qu, Y. Tian, R. Lu, and H. Liu, “Investigation on the metrology of conical thread gauge,” *Key Engineering Materials,* vol. 693, pp. 150–154, 2016.

[7] D. T. Maciel, S. L. M. R. Filho, C. H. Lauro, and L. C. Brandão, “Characteristics of machined and formed external threads in titanium alloy,” *International Journal of Advanced Manufacturing Technology,* vol. 79, no. 5–8, pp. 779–792, 2015.

[8] V. I. Leun and E. V. Nikolaeva, “Direct measurement of the mean thread diameter of cutting and monitoring tools in thread grinding,” *Russian Engineering Research,* vol. 35, no. 2, pp. 156–157, 2015.

[9] V. I. Leun and E. V. Nikolaeva, “Design of active monitoring systems for the mean thread diameter in thread grinding,” *Russian Engineering Research,* vol. 35, no. 4, pp. 313–314, 2015.

[10] W. Wu, D. Shao, W. Wang, and G. Wang, “Thread measurement algorithm research and software development,” *Key Engineering Materials,* vol. 579–580, pp. 392–397, 2014.

[11] C. Sheng, Z. Dongbiao, and L. Yonghua, “A new compensation method for measurement of thread pitch diameter by profile scanning,” *Measurement Science Review,* vol. 14, no. 6, pp. 323–330, 2014.

[12] S. Kosarevsky and V. Latypov, “Detection of screw threads in computed tomography 3D density fields,” *Measurement Science Review,* vol. 13, no. 6, pp. 292–297, 2013.

[13] E. Hong, H. Zhang, R. Katz, and J. S. Agapiou, “Non-contact inspection of internal threads of machined parts,” *International Journal of Advanced Manufacturing Technology,* vol. 62, no. 1–4, pp. 221–229, 2012.

[14] Y. Cheng, L. Bai, and L. Nie, “Enhanced high-precision and non-contact system for measuring geometrical size of the irregular shape,” *Advanced Science Letters,* vol. 6, pp. 625–628, 2012.

[15] I. A. Shchurov, “Calculation of the virtual pitch thread diameter using the cloud of points from CMM,” *International Journal of Advanced Manufacturing Technology,* vol. 53, no. 1–4, pp. 241–245, 2011.

[16] T. P. Merkač and B. Ačko, “Thread gauge calibration for industrial applications,” *Strojniski Vestnik/Journal of Mechanical Engineering,* vol. 56, no. 10, pp. 637–643, 2010.

[17] S. Kosarevsky and V. Latypov, “Development of an algorithm to detect screw threads in planar point clouds,” *Measurement Science Review,* vol. 10, no. 4, pp. 136–141, 2010.

[18] E. S. Gadelmawla, “A novel system for automatic measurement and inspection of parallel screw threads,” *Proceedings of the Institution of Mechanical Engineers, Part B: Journal of Engineering Manufacture,* vol. 218, no. 5, pp. 545–556, 2004.

[19] R. J. Hunsicker, J. Patten, A. Ledford, C. Ferman, M. Allen, and C. Ellis, “Automatic vision inspection and measurement system for external screw threads,” *Journal of Manufacturing Systems,* vol. 13, no. 5, pp. 370–384, 1994.

[20] M. R. Corley, E. E. Callens Jr, and H. G. Tull Iii, “Direct contact profile characterization of thread surfaces,” *Journal of Manufacturing Systems,* vol. 11, no. 5, pp. 309–313, 1992.

[21] R. Senthilnathan, M. Nandhini, R. Ranjani, and S. Sridevi, “Vision based orientation invariant measurement of metric screw thread parameters,” in *Proc. 9th International Conference on Trends in Industrial Measurement and Automation,* 2017.

[22] E. S. Gadelmawla, “Computer vision algorithms for measurement and inspection of external screw threads,” *Measurement: Journal of the International Measurement Confederation,* vol. 100, pp. 36–49, 2017.

[23] J. Chao and L. Zhang, “Parameters of small pitch thread measured by an intelligent detection method,” *Journal of Computational Methods in Sciences and Engineering,* vol. 16, no. 2, pp. 207–218, 2016.

[24] L. Zhao, H. Feng, and Q. Rong, “A novel non-contact measuring system for the thread profile of a ball screw,” *Mechanical Sciences,* vol. 9, no. 1, pp. 15–24, 2018.

[25] Y. C. Lee and S. S. Yeh, “Using machine vision to develop an on-machine thread measurement system for computer numerical control lathe machines,” *Lecture Notes in Engineering and Computer Science: Proceedings of The International MultiConference of Engineers and Computer Scientists 2019, IMECS 2019, 13-15 March, 2019, Hong Kong*, pp. 67–72.

[26] *ISO general purpose screw threads–Basic profile–Part 1: Metric screw threads,* I. O. F. Standardization ISO 68–1:1998.

[27] J. P. F. D'Haeyer, “Gaussian filtering of images: A regularization approach,” *Signal Processing,* vol. 18, no. 2, pp. 169–181, 1989.

[28] N. Otsu, “A threshold selection method from gray-level histograms,” *IEEE Transactions on Systems, Man, and Cybernetics,* vol. 9, no. 1, pp. 62–66, 1979.

[29] F. Shih, *Image Processing and Mathematical Morphology: Fundamentals and Applications*. New York, USA: CRC Press, 2009.

[30] J. Canny, “A computational approach to edge detection,” *IEEE Transactions on Pattern Analysis and Machine Intelligence,* vol. PAMI–8, no. 6, pp. 679–698, 1986.

[31] L. Cadena, A. Kruglyakov, F. Cadena, A. Romanenko, and A. Zotin, “Filters evaluation for detection of contours in satellite images for cadaster purposes,” *Lecture Notes in Engineering and Computer Science: Proceedings of The World Congress on Engineering and Computer Science 2017 Vol I, WCECS 2017, 25-27 October, 2017, San Francisco, USA*, pp. 422–425.

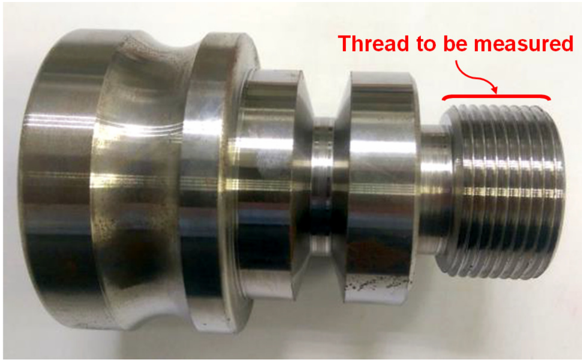

Fig. 1. Measured workpiece sample.

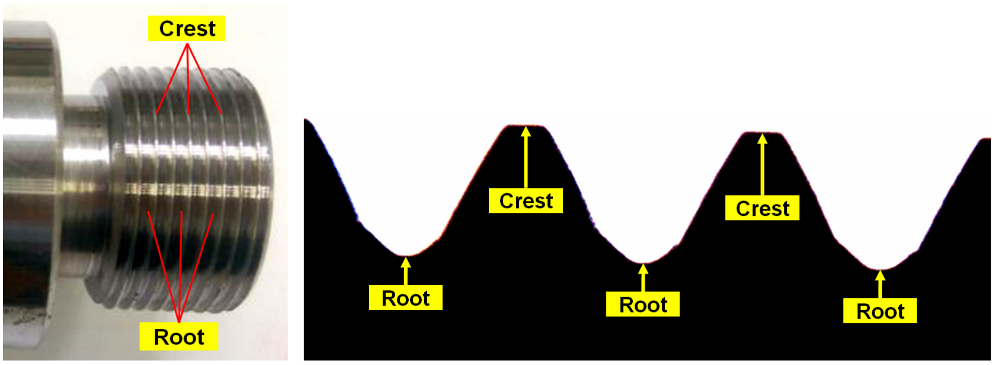

(a) Front-end threads of the sample (b) Front-end thread image

Fig. 2. Front-end threads of the sample and thread image.

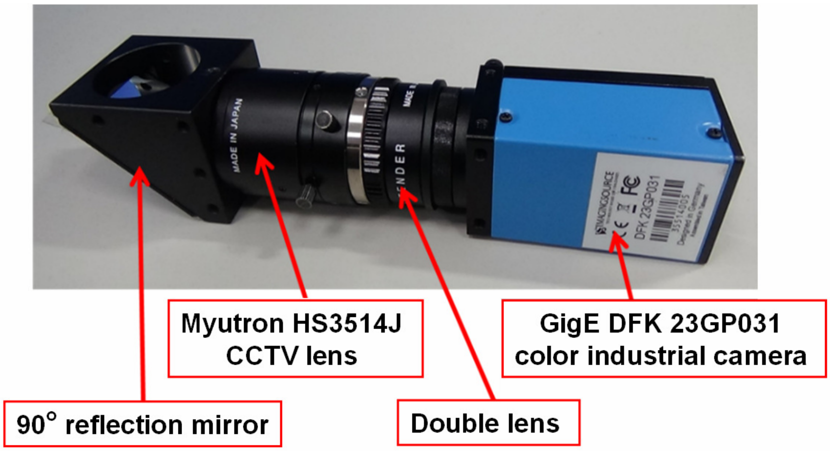

Fig. 3. Color industrial camera and lens-related components.

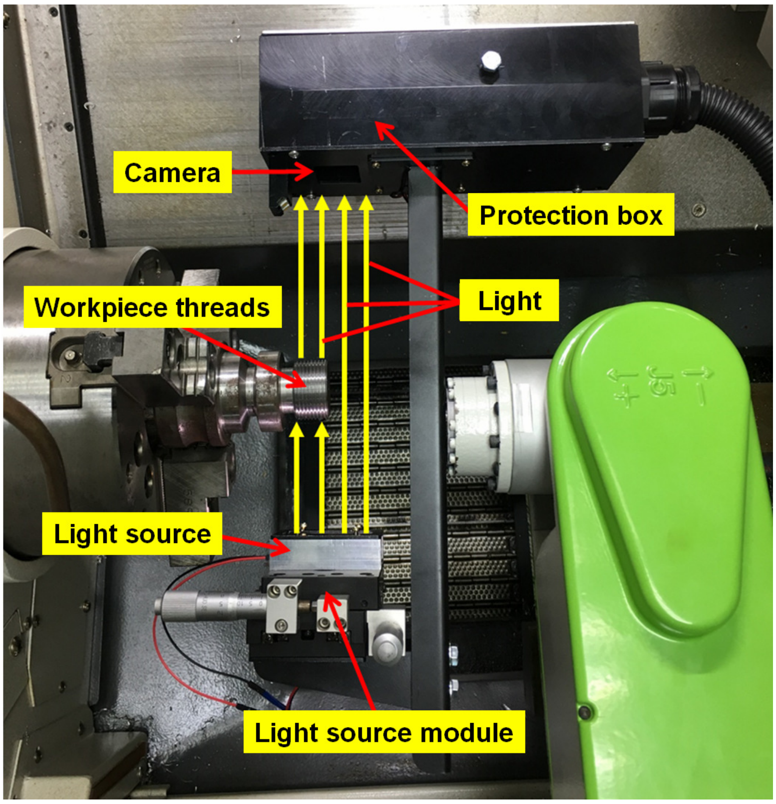

Fig. 4. Light source installation of the thread dimension measurement system.

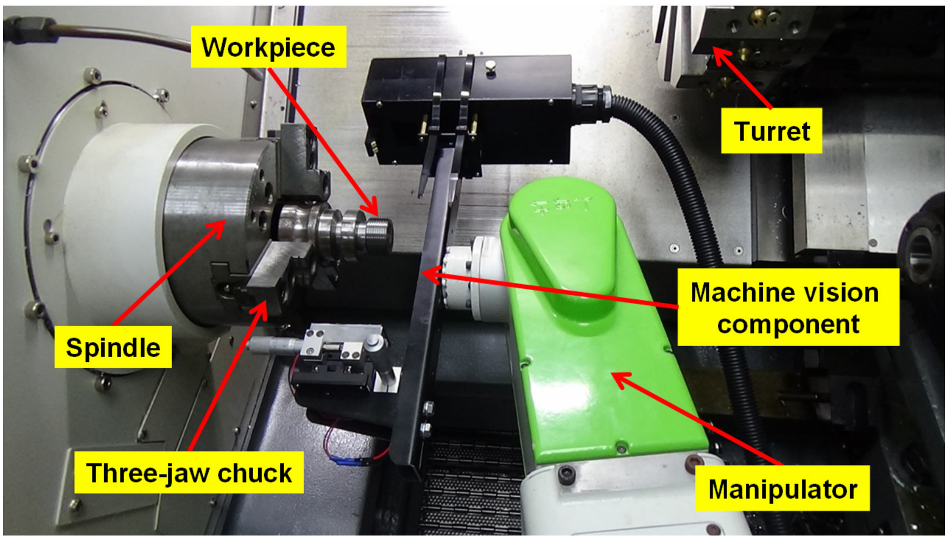

Fig. 5. Structure of the manipulator and machine vision components inside the lathe during the measuring process.

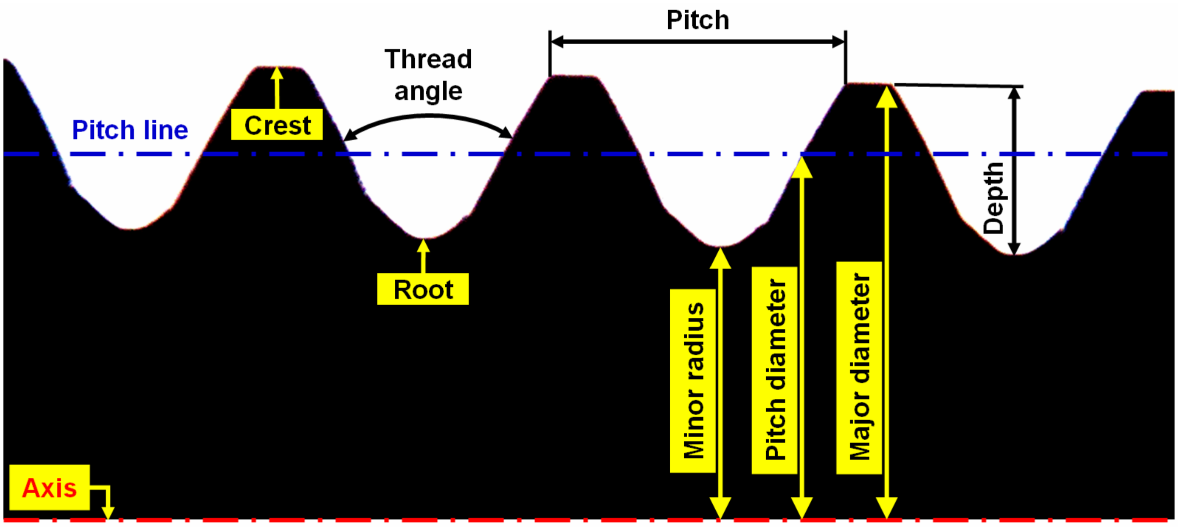

Fig. 6. Names of regions of threads.

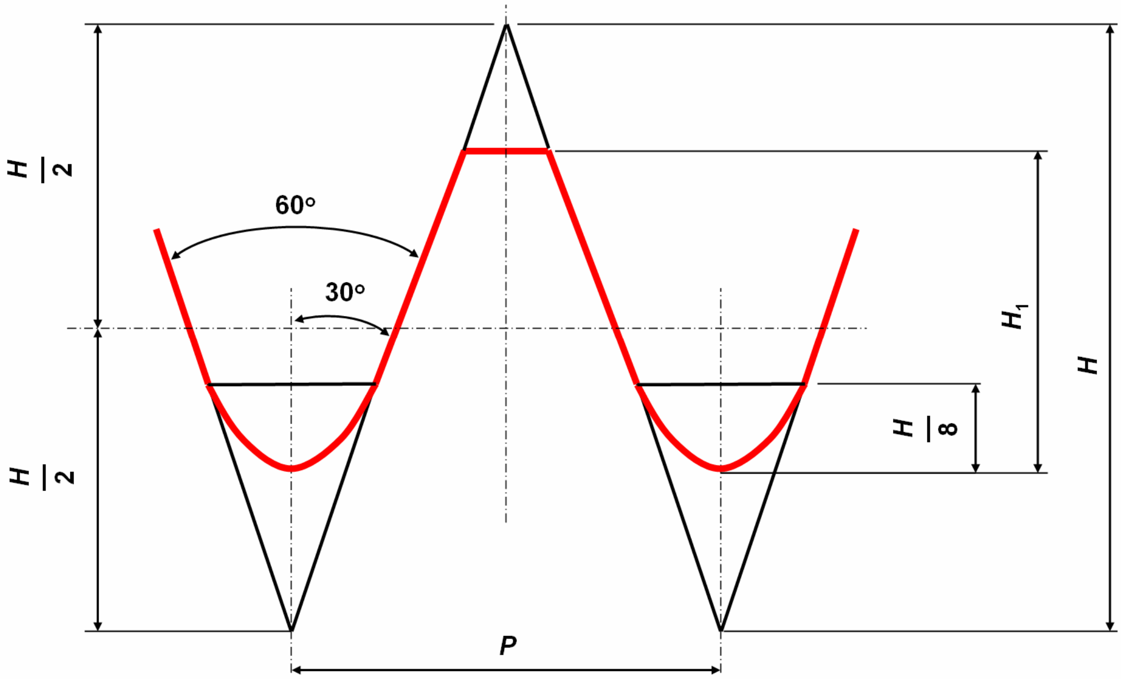

Fig. 7. Basic thread specifications [26] (this figure is redrawn based on Reference [26]).

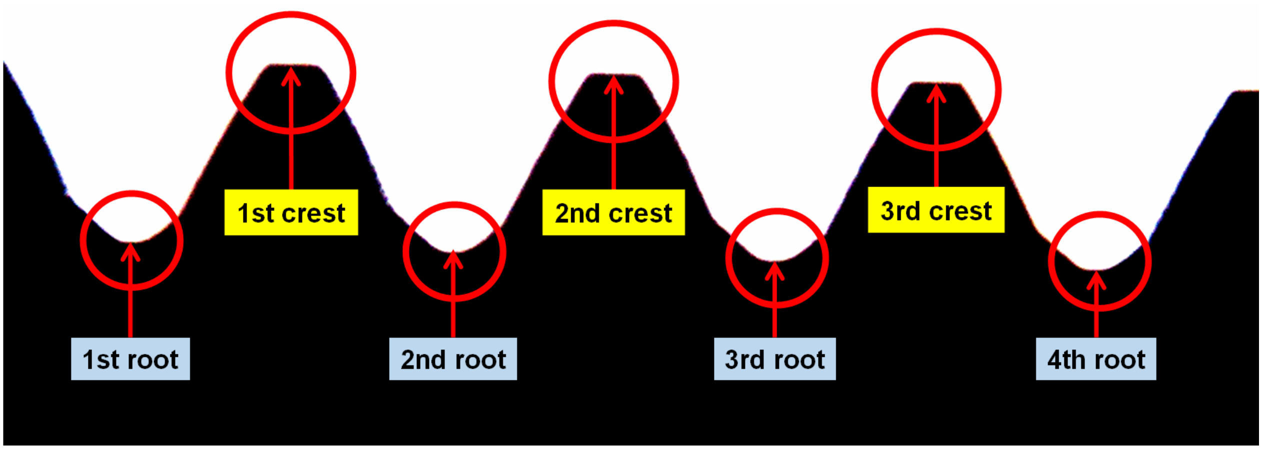

Fig. 8. Schematic of the crest and root in the thread images.

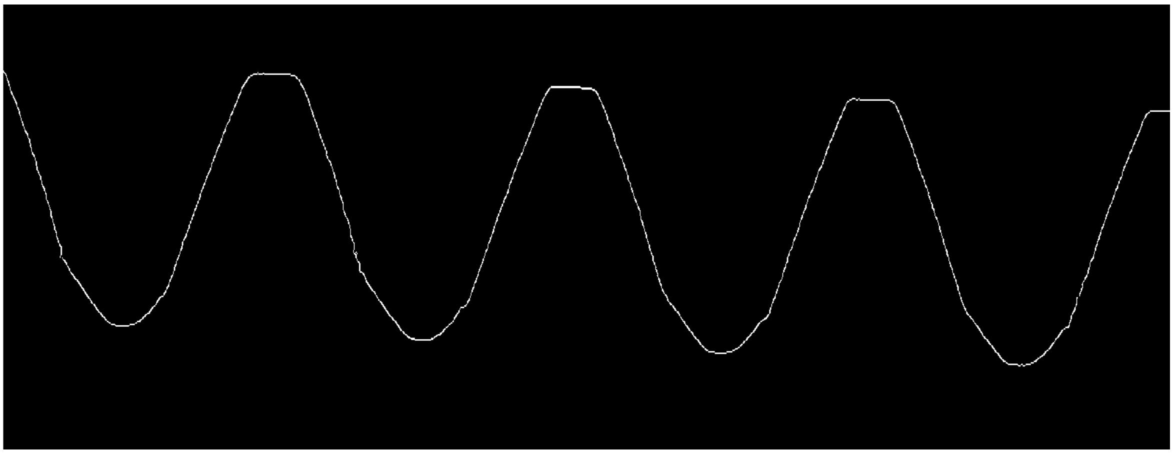

Fig. 9. Image after Canny edge detection.

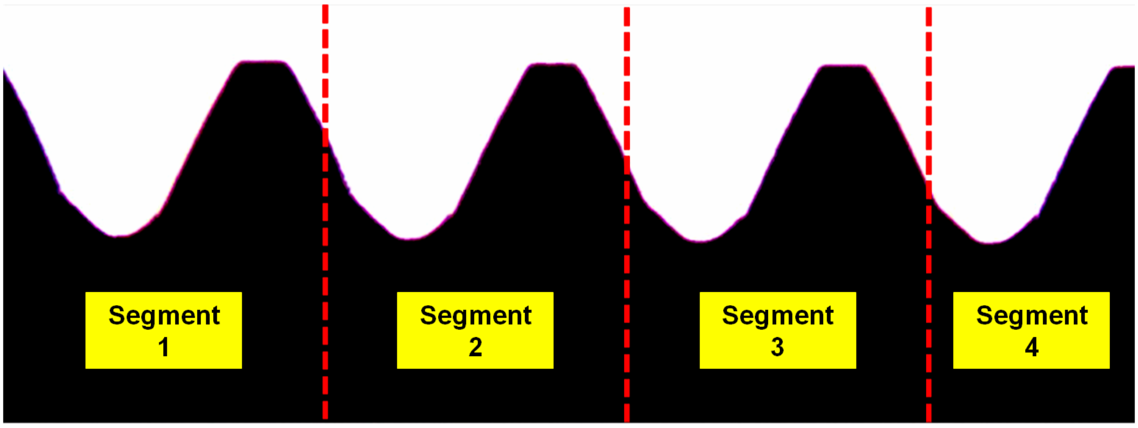

Fig. 10. Thread profile separated into four thread segments.

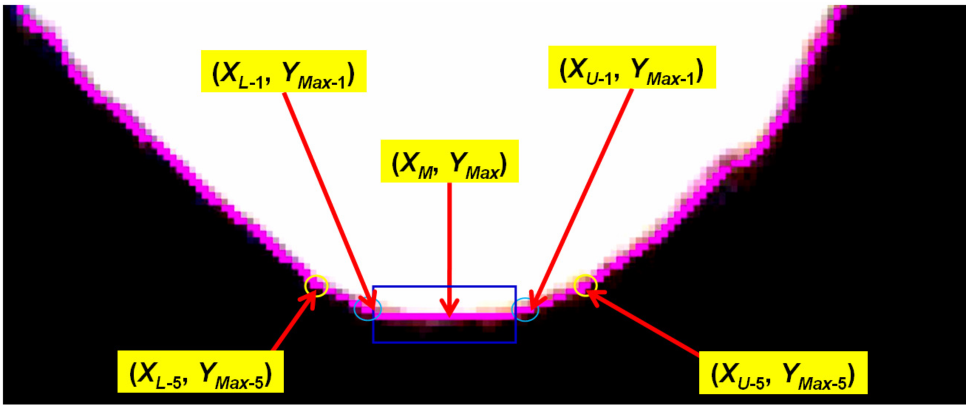

Fig. 11. Positions of the feature points in the thread pitch dimension calculation.

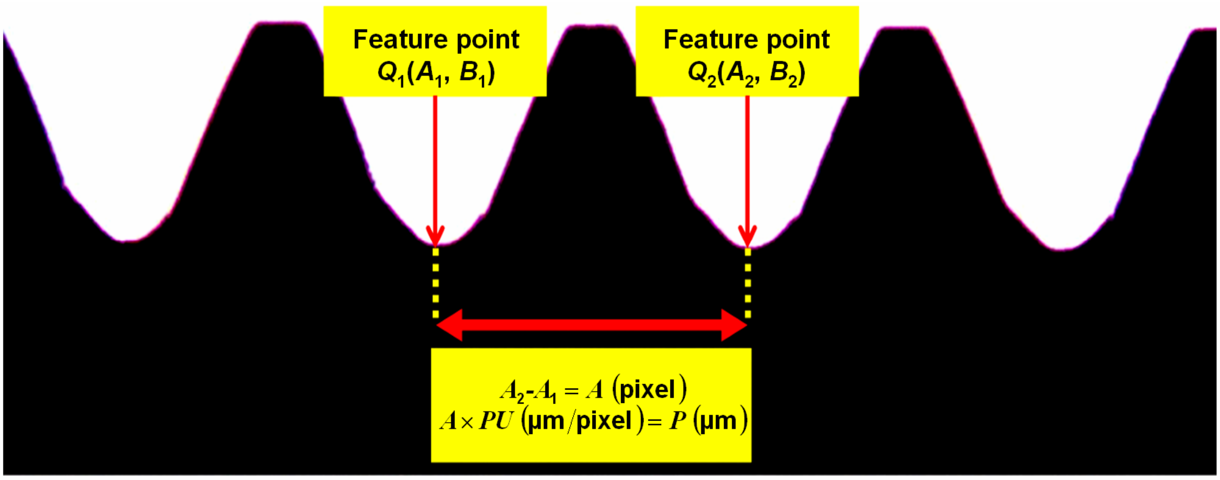

Fig. 12. Conversion of the thread pitch dimension.

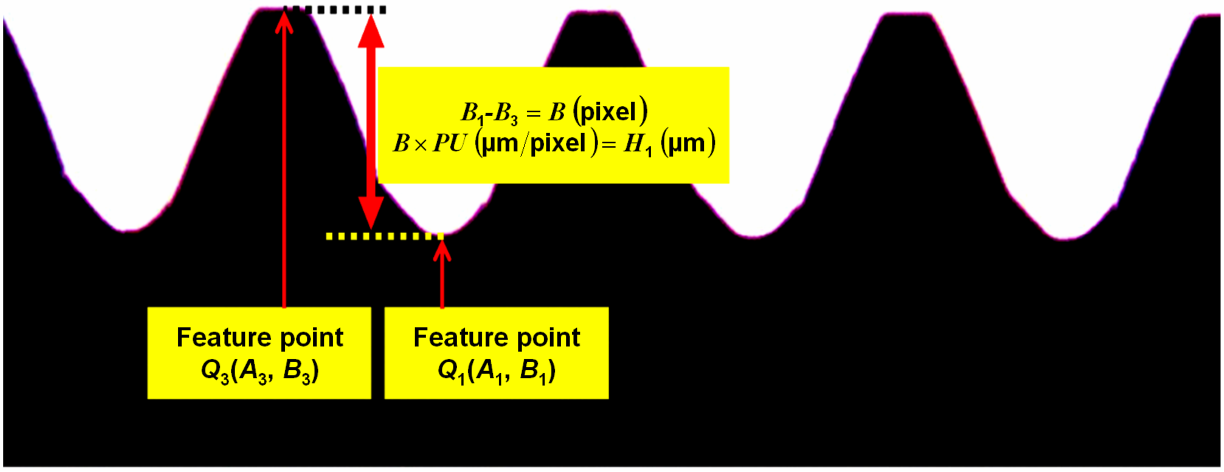

Fig. 13. Conversion of the thread depth dimension.

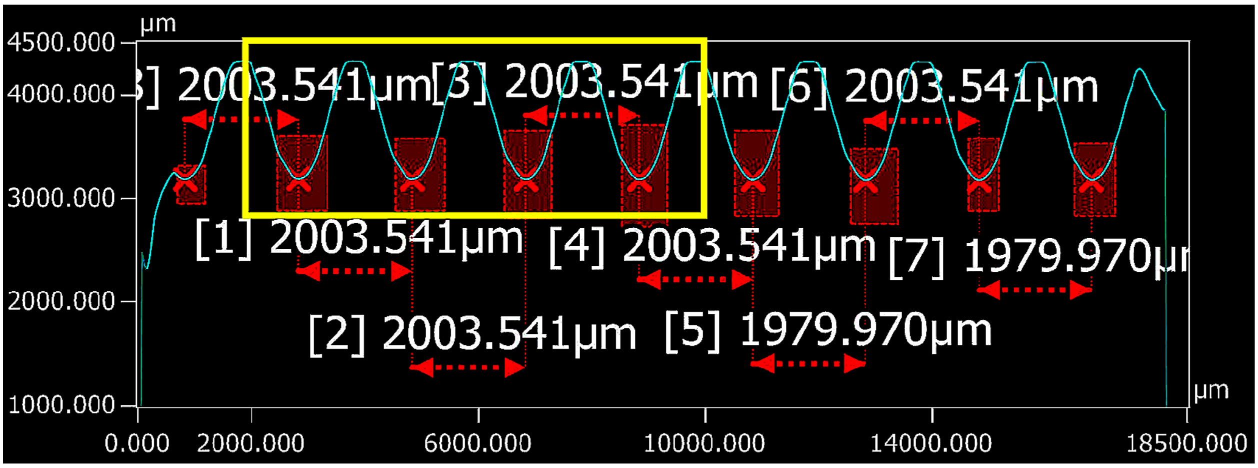

Fig. 14. Thread pitch result measured using a 3D microscope.

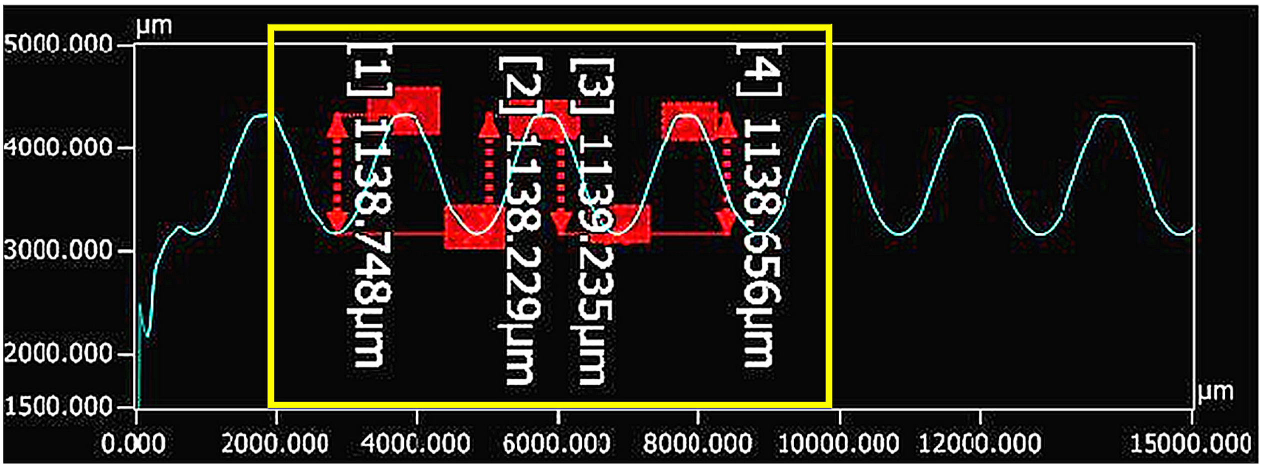

Fig. 15. Thread depth result measured using a 3D microscope.

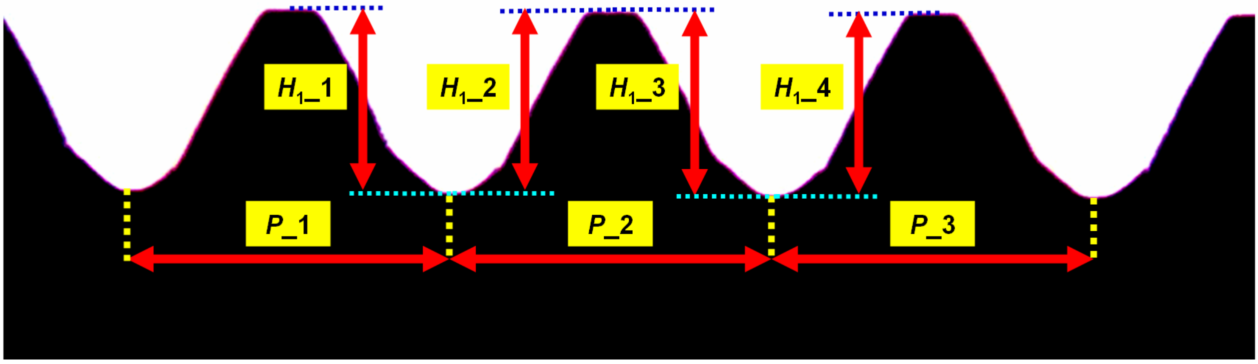

Fig. 16. Thread pitch and thread depth of the thread dimension measurement system.

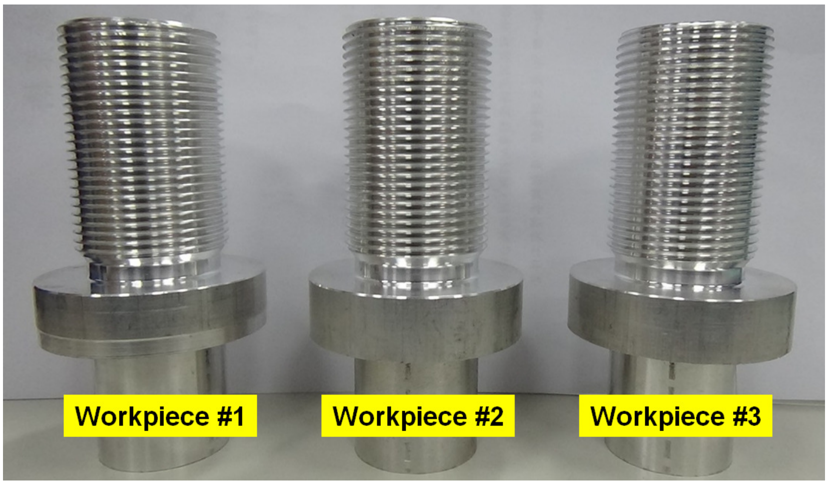

Fig. 17. Photograph of the workpiece samples.

TABLE I
$L_{18}(6^1 \times 3^5)$ ORTHOGONAL ARRAY

	T-hold	GF-Size	M-val	MT-Shape	MT-Size	MN-Times
L1	Otsu-40	3	3	R	3	3
L2	Otsu-40	5	4	C	5	5
L3	Otsu-40	7	5	E	7	7
L4	Otsu-20	3	3	C	5	7
L5	Otsu-20	5	4	E	7	3
L6	Otsu-20	7	5	R	3	5
L7	Otsu	3	4	R	7	5
L8	Otsu	5	5	C	3	7
L9	Otsu	7	3	E	5	3
L10	Otsu+20	3	5	E	5	5
L11	Otsu+20	5	3	R	7	7
L12	Otsu+20	7	4	C	3	3
L13	Otsu+40	3	4	E	3	7
L14	Otsu+40	5	5	R	5	3
L15	Otsu+40	7	3	C	7	5
L16	Otsu+60	3	5	C	7	3
L17	Otsu+60	5	3	E	3	5
L18	Otsu+60	7	4	R	5	7

TABLE II
EXPERIMENTAL MEASUREMENT ERROR RESULTS (UNIT: μm)

Thread dimension (error)	P_1 ($e_i^{P\_1}$)	P_2 ($e_i^{P\_2}$)	P_3 ($e_i^{P\_3}$)	H_1_1 ($e_i^{H_1\_1}$)	H_1_2 ($e_i^{H_1\_2}$)	H_1_3 ($e_i^{H_1\_3}$)	H_1_4 ($e_i^{H_1\_4}$)
Exp. 1	0.860	0.790	1.990	0.300	5.400	0.730	0.150
Exp. 2	1.180	0.400	1.970	0.300	5.400	0.260	0.320
Exp. 3	1.050	0.350	1.940	0.300	5.400	1.250	0.670
Exp. 4	1.000	0.300	2.560	0.300	5.400	0.950	0.370
Exp. 5	1.080	0.180	2.820	0.300	5.400	0.390	0.190
Exp. 6	0.930	0.040	2.630	0.300	5.400	0.950	0.370
Exp. 7	1.340	0.130	2.590	0.300	5.400	0.820	0.240
Exp. 8	0.690	0.190	2.250	0.300	5.400	1.060	0.480
Exp. 9	1.700	0.260	2.310	0.300	5.400	1.140	0.570
Exp. 10	1.360	0.050	2.530	0.300	5.400	0.390	0.190
Average μ	1.119	0.269	2.359	0.300	5.400	0.794	0.355
Standard deviation σ	0.290	0.219	0.314	0.000	0.000	0.344	0.174

TABLE III
MEASUREMENT RESULTS OF THE WORKPIECE SAMPLES (UNIT: μm)

Thread dimension	P_1	P_2	P_3	H_1_1	H_1_2	H_1_3	H_1_4
Workpiece #1	2008.165	2006.545	2008.164	1247.211	1247.187	1244.409	1243.811
Workpiece #2	2003.872	2014.533	2016.002	1257.323	1257.314	1257.314	1256.904
Workpiece #3	1997.111	2003.467	2014.418	1233.079	1234.124	1237.082	1238.621
Average (AVG)	2003.050	2008.181	2012.861	1245.871	1246.208	1246.269	1246.445
Difference of average (DA)	5.939	6.351	4.698	12.792	12.085	11.045	10.458
Ratio of the difference of average (RDA)	0.296%	0.316%	0.233%	1.027%	0.970%	0.886%	0.839%